J Mol Model (2013) 19:4459–4465
DOI 10.1007/s00894-013-1942-5

ORIGINAL PAPER

A DFT study of adsorption and decomposition of hexahydro-1,3,5-trinitro-1,3,5-triazine on Mg(0001) surface

Cai-Chao Ye · Feng-Qi Zhao · Si-Yu Xu · Xue-Hai Ju

Received: 19 May 2013 / Accepted: 9 July 2013 / Published online: 9 August 2013

Abstract The adsorption and decomposition of hexogen (RDX) molecule on the Mg(0001) surface were investigated by the generalized gradient approximation (GGA) of density functional theory (DFT). The calculations employed a supercell (4×4×4) slab model and three-dimensional periodic boundary conditions. The strong attractive forces between RDX molecule and magnesium atoms induce the RDX's N−O bond breaking. Subsequently, the dissociated oxygen atoms and radical fragment of RDX oxidize the Mg surface. The largest adsorption energy is −2104.0 kJ mol^{-1}. We also investigated the decomposition mechanism of RDX molecule on the Mg(0001) surface. The activation energy for the dissociation step of configuration **V4** is as small as 2.5 kJ mol^{-1}, while activation energies of other configurations are much larger, in the range of 964.9–1375.1 kJ mol^{-1}. Mg powder is more active than Al powder, and Mg powder performs better in increasing the combustion exothermicity of RDX as well.

Keywords Adsorption and dissociation · Density functional theory · Hexahydro-1,3,5-trinitro-1,3,5-triazine (RDX) · Mg(0001) surface

C.-C. Ye · X.-H. Ju (✉)
Key Laboratory of Soft Chemistry and Functional Materials of MOE, School of Chemical Engineering, Nanjing University of Science and Technology, Nanjing 210094, People's Republic of China
e-mail: xhju@mail.njust.edu.cn

F.-Q. Zhao · S.-Y. Xu
Science and Technology on Combustion and Explosion Laboratory, Xi'an Modern Chemistry Research Institute, Xi'an 710065, People's Republic of China

Introduction

Burning in air, magnesium produces a brilliant white light which includes strong ultraviolet. This property was used in incendiary weapons, firebombing and an additive agent in conventional propellants [1, 2]. Hexogen (RDX), hexahydro-1,3,5-trinitro-1,3,5-triazine ($C_3H_6N_6O_6$), is a well-known explosive compound, typical high energetic density material (HEDM) [3, 4], has been widely used in solid propellant as oxygenant. As the metallic magnesium is also incorporated in explosives to raise reaction temperatures and create incendiary effects, it is important to understand the reaction in RDX/Mg composite propellants [5]. However, the study on the interaction of energetic materials and magnesium is lacking at present. Although there are some research works of H_2 on the magnesium surface [6, 7], there is no report of RDX on the magnesium surface. To clarify some of the fundamental issues related to the interaction of energetic materials, especially nitro compounds, on the Mg surface, we focused on the atomic-level description of the interaction between the energetic compound of RDX and Mg surface.

Recently, we studied the adsorption and decomposition of the 1,1-diamino-2,2-dinitroethylene (FOX-7), RDX and nitroamine molecules on Al(111) surface by density functional theory [8–10]. The oxidation of the aluminum surface readily occurs by partial or complete dissociation of the oxygen atoms from the NO_2 groups in FOX-7, RDX and nitroamine. In the case of dissociative chemisorption, absorption of one or both O-atoms of a nitro group and decomposed NO_2 group by Al surface atoms was the dominant mechanism. What is the difference when the Al surface is replaced by magnesium? To answer this question, we investigated the adsorption and decomposition of RDX on the Mg surface.

In this paper, we reported five adsorption configurations of RDX on Mg(0001) surface. In addition to studying the

geometries and energies of adsorptions, we investigated the density of states. In view of the fact that the DFT calculations were employed to investigate the chemisorptions and dissociation pathways of NO on the Rh surfaces [11] as well as H_2S on the closed packed surfaces of a number of important noble metals and transition metals [12, 13], we also studied the decomposition mechanism of RDX molecule on the Mg(0001) surface.

Computational methods

The calculations described in this paper have been performed using the CASTEP package [14] with Vanderbilt-type ultrasoft pseudopotentials [15, 16] and a plane-wave expansion of the wave functions. Exchange and correlation were treated with the generalized gradient approximation, using the functional form of Perdew, Burke, and Ernzerhof of PBE [17]. The electronic wave functions were obtained by a density-mixing scheme [18] and the structures were relaxed using the Broyden, Fletcher, Goldfarb, and Shannon (BFGS) method [19]. The cutoff energy of plane waves was set to 340.0 eV. Brillouin zone sampling was performed using the Monkhost–Pack scheme. The values of the kinetic energy cutoff and the k-point grid were determined to ensure the convergence of total energies.

The experimentally-determined crystal structure of Mg was used to construct the slab for this study [20]. Since the surface energy of Mg(0001) is the smallest [21, 22], we choose Mg(0001) surface to investigate the adsorption and decomposition of RDX on the Mg surface. The magnesium surface was represented by a slab model with periodic boundary conditions. Particularly, a 4×4 supercell with four layers containing 64 Mg atoms was used to study the adsorption of the molecular systems (Fig. 1). The slabs were separated by 17 Å of vacuum along c axes direction for the case with RDX molecule. The cell size with rhombic box of a×b×c is 12.84 Å×12.84 Å×25.82 Å. In calculations of molecular adsorption on the surface, we have relaxed all atomic positions of the RDX molecule, as well as the Mg atoms of the slab.

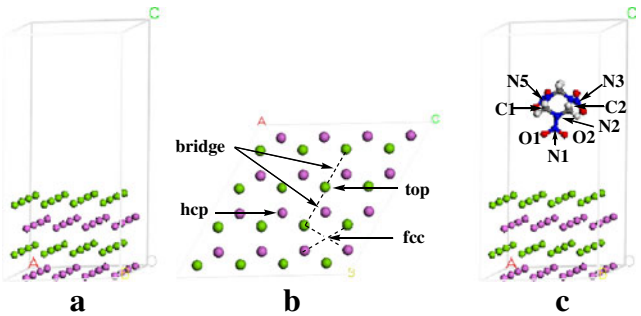

Fig. 1 **a** Lateral view of the slab model of Mg(0001). Atoms in different layers are colored differently for easy identification. **b** Top view of the surface. Surface sites are depicted in the panel. **c** RDX molecule on the Mg surface with no interactions

Several tests have been performed to verify the accuracy of the method when applied to bulk magnesium and to the isolated RDX molecules, such as the optimum cutoff energy for calculations. For bulk magnesium, the 2-atom rhombohedral primitive cell has been optimized using a cutoff energy of 340 eV. We have tested for convergence, using the *k*-point sampling density and the kinetic energy cutoff. When a cutoff energy is 340 eV, a Monkhorst-Pack scheme with mesh parameters of 9×9×6 has been used, leading to 36*k*–points in the irreducible Brillouin zone. Based on this calculation, the optimized rhombohedral unit parameters are a_{calc}= b_{calc}=3.23 Å, and c_{calc}=5.19 Å. When a cutoff energy is 380 eV, the obtained rhombohedral unit parameters are a_{calc}=b_{calc}=3.22 Å, and c_{calc}=5.17 Å. The difference of unit parameters is very small when the cutoff energy changes from 340 eV to 380 eV. It can be concluded that, at E_{cut}=340 eV, the bulk structure is well converged, with respect to the cutoff energy. The calculated lattice constants of 3.23 Å and 5.19 Å are very close to the experimental values (a_{exp}= 3.21 Å, c_{calc}=5.21 Å) [20]. These results indicate that the present sets of pseudo-potentials are able to provide a very good representation of the structural properties of bulk magnesium.

An equally good representation has been observed for the geometric parameters of the isolated RDX molecules. For example, on the basis of optimizations of the isolated RDX molecule in a rhombic box with dimensions of 12.84 Å× 12.84 Å×25.82 Å, the calculated geometries were listed in Table 1. As can be seen from Table 1, we noticed that there are no significant differences between the values from two different cutoff energies, indicating convergence of the results even at E_{cut}=340 eV. These values are also similar to the experimental data for crystal RDX [23]. However, the calculated N-N distances differ from the experimental value (0.05 A).

The good agreement between our calculated properties of magnesium bulk and the isolated RDX molecule with the experiment enable us to proceed to the next step: the investigation of molecular adsorption on the Mg(0001) surface. This also suggests that the performed computational method

Table 1 Geometric parameters of the isolated RDX molecules obtained from optimizations at two cutoff energies and experimental data

Geometries	E_{cut}=340 eV	E_{cut}=380 eV	Exp. [a]
r (N1−N2)	1.417 Å	1.415 Å	1.36 Å
r (N1−O1)	1.248 Å	1.249 Å	1.23 Å
r (N1−O2)	1.248 Å	1.248 Å	1.23 Å
θ (N1−N2−C1)	119.7°	119.6°	118.7°
θ (N1−N2−C2)	119.6°	119.7°	118.7°

[a] data from ref [23]

is proper to the adsorption system of RDX molecule on the Mg(0001) surface. In calculations of molecular adsorption on the surface, we have relaxed all atomic positions of the molecule, as well as the Mg atoms of the slab.

For the case of adsorption configurations, the corresponding adsorption energy (E_{ads}) was calculated according to the expression.

$$E_{ads} = E_{(adsorbate+slab)} - E_{(molecule+slab)} \quad (1)$$

,where $E_{(adsorbate\ +\ slab)}$ is the total energy of the adsorbate/slab system after the RDX molecule being absorbed by Mg slab and $E_{(molecule\ +\ slab)}$ is the single-point energy of the RDX/slab system as a whole but without interactions between RDX molecule and the Mg slab (RDX is as far as 6.78 Å away from the top-Mg atom of Mg surface).

The $E_{(adsorbate+slab)}$ and $E_{(molecule+slab)}$ were calculated with the same periodic boundary conditions and the same Brillouin-zone sampling. A negative E_{ads} value corresponds to a stable adsorbate/slab system. Figure 1 shows the pictorial view of the Mg(0001) surface model, the absorbed surface sites and the configuration of RDX molecule on the Mg(0001) surface with no adsorbate-Mg interactions.

Transition states (TS) were located by using the complete LST/QST method [24]. Firstly, the linear synchronous transit (LST) maximization was performed, followed by an energy minimization in directions conjugated to the reaction pathway. The TS approximation obtained in that way was used to perform quadratic synchronous transit (QST) maximization. From that point, another conjugate gradient minimization was performed. The cycle was repeated until a stationary point was located. The convergence criterion for transition state calculations was set to 0.05 eV/Å for the root-mean-square forces. The activation energy is defined as $E_a = E_{TS} - E_R$, where E_{TS} is the energy of transition state, and E_R is the sum of the energies of reactants.

Results and discussion

The adsorption and decomposition of RDX molecule on the Mg(0001) surface are very complicated. There exist both physical and chemical adsorptions, and the latter result in the decomposition of the RDX molecule on the Mg surface. There are four cases as Eqs. (1) to (4).

(1) The RDX molecule is nondissociative, for example, see **V4** and **P1** in Fig. 2

(2) 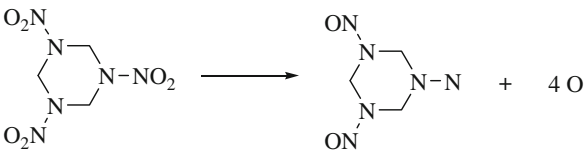

see **V1** in Fig. 2

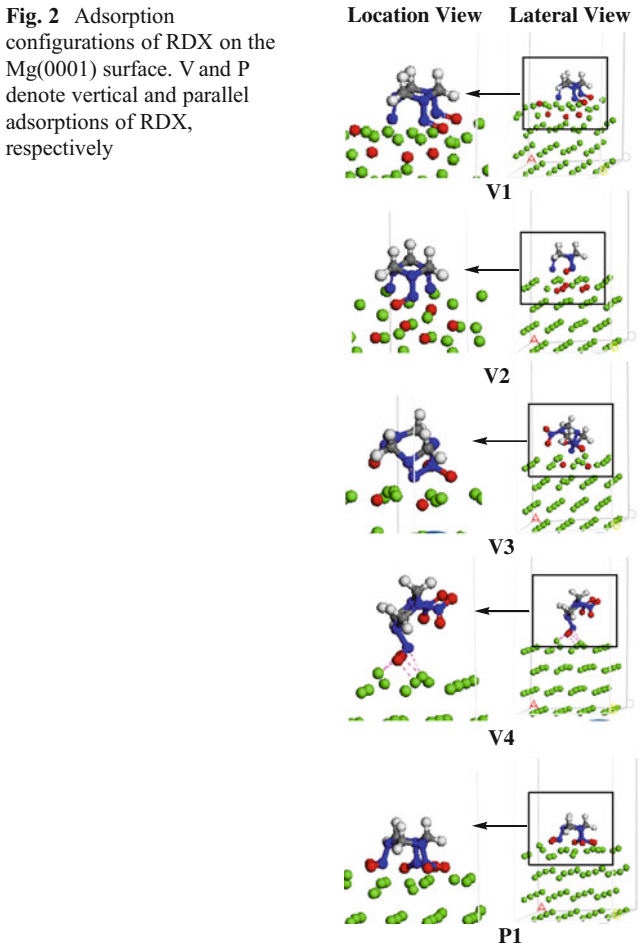

Fig. 2 Adsorption configurations of RDX on the Mg(0001) surface. V and P denote vertical and parallel adsorptions of RDX, respectively

(3) 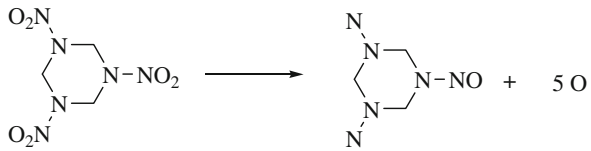

see **V2** in Fig. 2

(4) 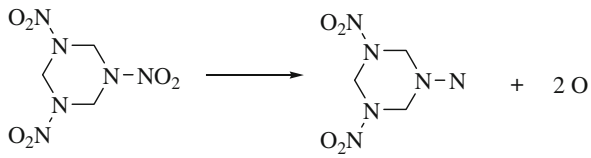

see **V3** in Fig. 2

According to the orientation of the RDX molecule relative to the Mg(0001) surface, **V** and **P** denote vertical and parallel adsorptions of RDX, respectively. The lateral views of the optimized adsorption configurations after full relaxation of the atomic positions were shown in Fig. 2.

Geometries

The adsorption energies were calculated by Formula (1) and given in Table 2. As can be seen in Fig. 2, the N1−N2 bond is initially vertical to the Mg surface and above an on-top site, an hcp site, a bridge site, and an fcc site **for V1** to **V4** configurations, respectively. **P1** is the adsorption configuration that RDX molecule was initially parallel to the Mg surface. Adsorption at **V1** to **V3** sites lead to dissociations of O atoms of nitro groups, which decomposed as Eqs. (2) to (4). The RDX fragments and dissociated O atoms adsorb on the Mg surface, resulting in formation of Mg–O and Mg–N bonds. For **V1** to **V3** configurations, the number of newly built Mg−O bonds is 20, 22, 12, respectively, as well as the number of Mg–N bonds between RDX fragment and Mg atoms is 5, 6, 4, respectively. The Mg−O and Mg–N bonds are in the lengths of 2.031−2.213 Å and 2.016−2.191 Å, respectively. In addition, a ring structure with five atoms is formed in **V3** configuration, this is due to the fact that two O atoms on N1 atom dissociated, and that the N1 atom moves close to N3 atom to form an N–N bond (1.579 Å) with a cyclization. **V4** and **P1** are the adsorption configurations of non-dissociative RDX. For **V4**, there are four close Mg−O distances of 2.039–2.138 Å. For **P1**, there are 12 close Mg−O distances of 2.006−2.214 Å and three close Mg−N distances of 2.153−2.463 Å. In addition, for all adsorption configurations, except that the Mg atoms with O or N atoms strongly interact to form Mg−O and Mg–N bonds, the other Mg atoms almost keep their original positions.

In a word, the RDX molecule decomposes to different products due to the interacting of RDX molecule and Mg atoms, resulting in strongly chemical adsorptions. Besides the formation of strong Mg−O bonds, the Mg−N bonds also form through the strong interaction of nitro N atoms with the surface Mg atoms. The radical species obtained as a result of N−O bonds dissociation remain bonded to the Mg(0001) surface.

Adsorption energies

As can be seen from Table 2 and Fig. 2, the E_{ads} value of **V4** (−220.7 kJ mol^{-1}) is the smallest, since the RDX molecule is not decomposed, the strong interaction between Mg surface and one NO_2 group results in four Mg−O bonds. Similarly, the E_{ads} value of **P1** (−698.6 kJ mol^{-1}) is the second smallest, since the RDX molecule is parallel to Mg surface and not decomposed, the strong interaction between Mg surface and three NO_2 group results in 12 Mg−O bonds, as well as three Mg−N bonds. When two N−O bond in one NO_2 group of RDX molecule decompose, the corresponding adsorption energy of **V3** is −959.8 kJ mol^{-1}. For the adsorption configurations of four and five N−O bonds dissociated, i.e., **V1** and **V2**, their adsorption energies are −1731.0 and −2104.0 kJ mol^{-1}, respectively. Compared with the adsorption energies of RDX/Al(111) system (in the range of −293.1 to −835.7 kJ mol^{-1}) [10], the E_{ads} value of RDX/Mg(111) system is more negative. Based on the adsorption energies of the RDX on the Mg(0001) surface, it can be concluded that the interacting of the RDX molecule and Mg atoms is very strong and the chemical adsorption is dominant. Mg powder is more active than Al powder and Mg powder performs better in increasing the combustion exothermicity of RDX as well.

Table 2 Adsorption energies (E_{ads}), activation energies (E_a) and adsorption sites of RDX on the Mg(0001) surface

Relation of plane of RDX molecule with the Mg surface	Configurations	Adsorption sites	E_{ads} (kJ mol^{-1})	E_a (kJ mol^{-1})
vertical	**V1**	Top	−1731.0	–
	V2	hcp	−2104.0	964.9
	V3	Bridge	−959.8	1375.1
	V4	fcc	−220.7	2.5
parallel	**P1**	Level	−698.6	–

Density of state (DOS)

The electronic structure is intimately related to their fundamental physical and chemical properties. Moreover, the electronic structures and properties are related to the adsorptions and decompositions for the adsorbates. The discussion above suggests that the decomposition of the RDX molecule on the Mg surface initiates from the rupture of N−O bond and results in the formation of Mg−O and Mg−N bonds. Therefore, the knowledge of their electronical properties appears to be useful for further understanding the behaviors of the RDX molecule on the Mg surface. Figure 3 displays the calculated partial DOS (PDOS) from −25 to 5 eV for all adsorption configurations. For comparison, the PDOS of the free RDX molecule and Mg surface were also shown in Fig. 3. The electronic structures vary with adsorption configurations due to the differently dissociated products of the RDX molecule.

As can be seen from Fig. 3, the PDOS peaks change greatly in **V1** to **V3** configurations, as compared to the configuration in which there is no RDX/Mg interaction. The values of the peaks become smaller, while the number of the peaks increases, which indicates that the stability of RDX and Mg surface declines greatly and the activity increases. For **V1** to **V3**, after adsorption, the RDX molecules decompose into RDX fragments and O atoms. For N atoms, because of Mg−N bonds formed, the PDOS peaks are mostly overlapped with peaks of Mg atoms in range of −7.5 to 2.5 eV, and the number of the peaks increases almost twice. For O atoms, as a large number of Mg-O bonds form, these highest PDOS peaks of O atoms of **V1** to **V3** become smaller

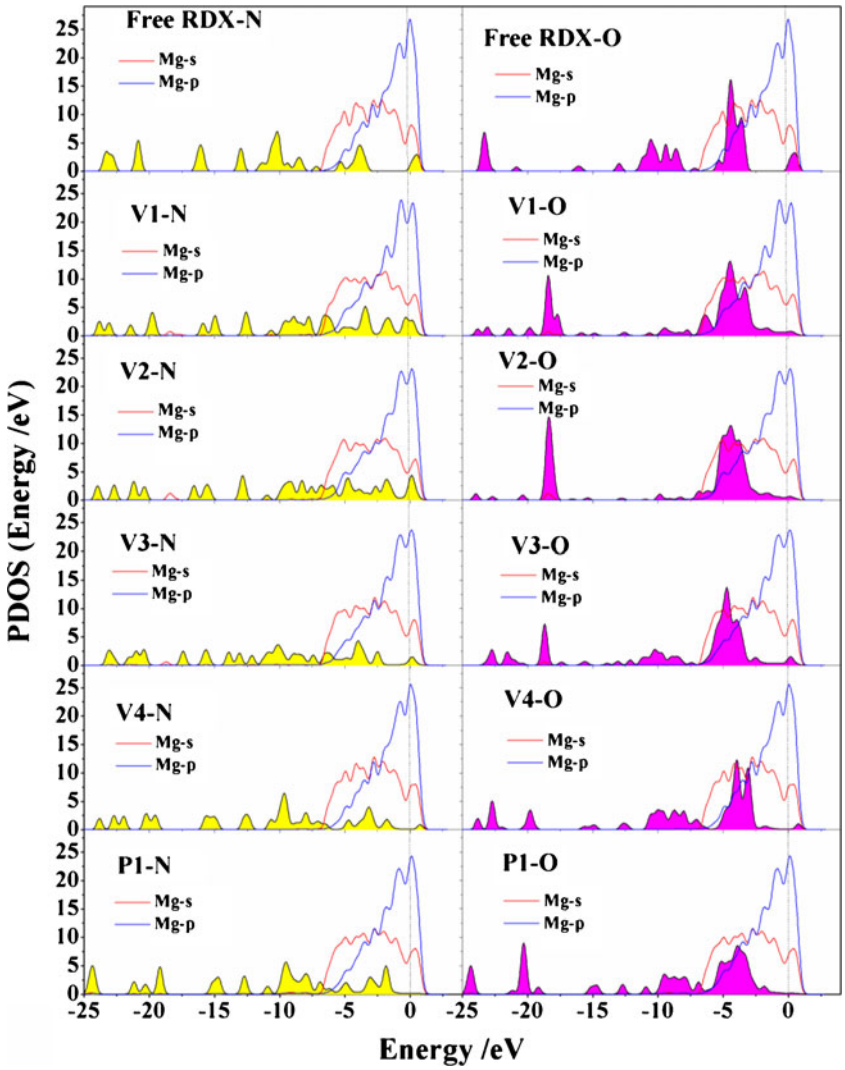

Fig. 3 The PDOS for the RDX molecule and the absorbed Mg atoms. The area filled with yellow color represents PDOS of N atoms and the area filled with pink color represents PDOS of O atoms. The Fermi energy is set to zero

and shift down slightly, and the peaks become smoother, whereas the PDOS peaks disappeared in the range of −12.5 to 7.5 eV. The highest PDOS peak of O atoms overlap completely with the peaks of Mg atoms at −7.5 to 0 eV. For **V4**, as the RDX molecule is nondissociated during the adsorption process, the peaks of the PDOS projection on N atoms is similar to those of free RDX, and the peaks of O atoms become smoother in the range of −12 to −6 eV. Finally, in **P1** configuration, both for N and O atoms, the values of the peaks become smaller, and the number of the peaks increases. It is because the RDX molecule is parallel to the Mg surface and oxidizes the Mg surface with 12 similar Mg−O bonds and three Mg−N bonds.

It is remarkable that a new peak appears at the energy of −18.5 eV in PDOS projection on O for five configurations discussed above. The value of peak in **V2** is largest (22 Mg−O bonds formed), followed by **V1** (20 Mg−O bond formed)>**P1** (12 Mg−O bonds formed)>**V3** (12 Mg−O bond formed)>**V4** (four Mg−O bonds formed). Hence, the new peaks can be attributed to the formation of Mg−O bonds, and the greater the degree of oxidized Mg surface, the larger the value of peak.

For all adsorption configurations, the DOS of Mg atoms changes slightly. At the range of −7.5 to 2.5 eV, the DOS of Mg atoms with N and O atoms overlap in different degrees. From the above analysis we can concluded that when bonding interactions between the absorbates and the Mg surface are strengthened, the PDOS shifts and becomes smoother with respect to those of free RDX molecule. And this shows that the strong interaction between RDX and Mg results in the overlaps of the electronic outer orbitals between Mg and O or N atoms of RDX.

The mechanism of dissociation

The reactants (**R**), transition state (**TS**) and products for the surface reaction of RDX molecule on the Mg(0001) were depicted in Fig. 4, and a detailed energy profile for three

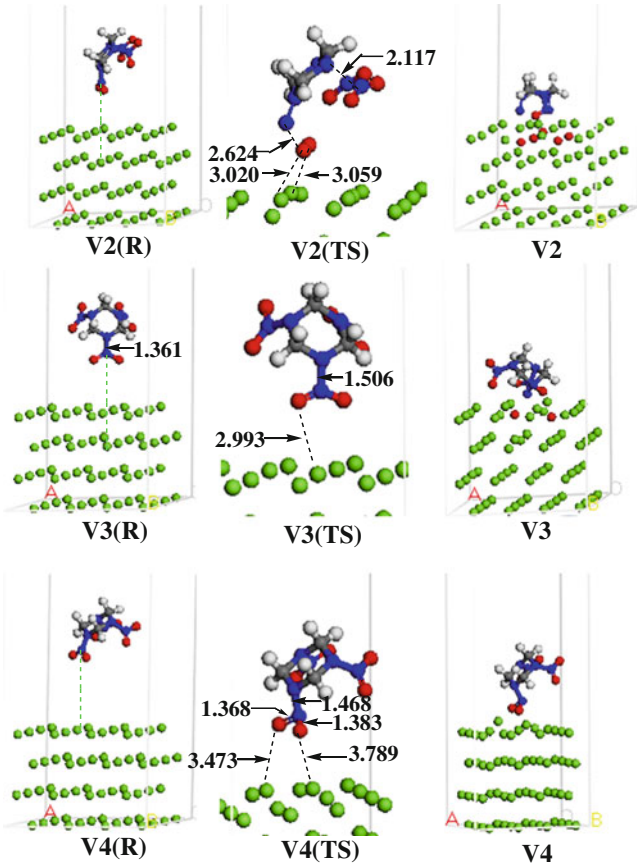

Fig. 4 Lateral views of RDX on the Mg(0001) surface. The index R and TS denote the reactant and transition state, respectively

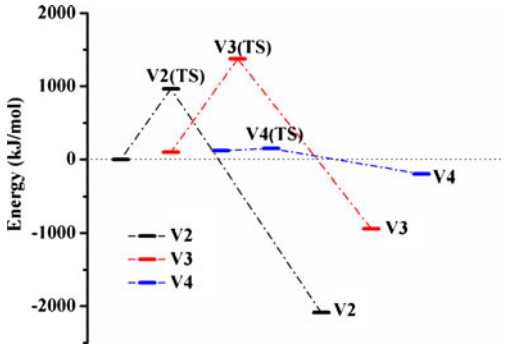

Fig. 5 Relative energy profile for RDX decomposition on the Mg(0001) surfaces

dissociations of adsorbed RDX configurations were presented in Fig. 5. The activation energies at transition state and interaction energies were tabulated in Table 2.

As can be seen from Fig. 4, the RDX molecule interacts with several Mg atoms that deviate from the Mg surface obviously for **V2(TS)**. The O1 and O2 atoms move away from N1 atom, as the distance between N1 and O2 increases from 1.218 to 2.624 Å, while the distance between N1 and O1 increases from 1.225 to 1.789 Å. At the same time, the N3 and N5 nitro groups move away from RDX molecule and the distance between N3 and N4 increases from 1.395 to 2.117 Å, while the distance between N5 and N6 increases from 1.404 to 1.945 Å. The activation energy (E_a) of this transition state is 964.9 kJ mol^{-1} (see Table 2 and Fig. 5), indicating that this process is very hard to occur. In the decomposition process, all the O atoms keep moving to the Mg surface and the entire N−O bonds are broken except N3−O3 bond. These dissociated O atoms bind with the surface Mg atoms and form 22 Mg−O bonds. In addition, another six Mg−N bonds come into being. For **V3(TS)** and **V4(TS)**, the RDX molecule does not decompose in these two species, as compared to the local minimum of physical adsorptions, the RDX molecule moves down toward the Mg surface and interacts with surface Mg atoms. As a result, some Mg atoms deviate from the Mg surface obviously. Compared to the initial state, the bond length of N1−N2 bond in **V3(TS)** increases from 1.361 to 1.506 Å and those in **V4(TS)** increases from 1.403 to 1.463 Å. In **V3,** with the reaction going on, two O atoms dissociated from N1 atoms. The activation energies (E_a) are 1375.1 kJ mol^{-1} (this process hardly occurs). After the transition state, the N1−O1 and N1−O2 bonds rupture. The dissociated moiety binds to the surface and forms 12 Mg−O bonds. The activation energy is so large that the RDX molecule does not decompose via **V3(TS)**. Compared to the local minimum of physical adsorption, the RDX molecule moves toward the Mg surface and attracts several Mg atoms that deviate from the Mg surface obviously. In **V4(TS)** the bond lengths of N1−O1 and N1−O2 increase from 1.250/1.250 to 1.368/1.383 Å, while the distances between the O1 atoms and the nearest Mg atoms decrease from 6.757 to 3.473 Å. The activation barrier (E_a) of **V4(TS)** is 2.5 kJ mol^{-1}, which means that this process is easy to occur. Through **V4(TS)**, the RDX molecule forms four Mg−O bonds (see **V4**).

Conclusions

Based on the investigation of RDX molecule on Mg(0001) surface, the major findings can be summarized as follows.

1. There exist physical as well as chemical adsorptions when the RDX molecule approaches the Mg surface. The Mg surface is readily oxidized by the oxygen-rich nitro group of the dissociatively adsorbed RDX. Dissociations of N−O bonds of nitro group result in the formations of strong Mg−O and Mg−N bonds. As the number of the formations of Mg−O and Mg−N bonds increases, the corresponding adsorption energy increases greatly.
2. The PDOS projections on the N and O atoms for the dissociated N−O bonds adsorptions occur with an obvious shift of peaks, which infers that energy bands become broad and the interactions of chemical bonds are

strengthened. When bonding interactions between the absorbates and the Mg surface are strengthened, the PDOS shifts and becomes smoother with respect to those of free RDX molecule (without interaction with Mg). The strong interaction between RDX and Mg results in the overlaps of the electronic outer orbitals between Mg and O or N atoms of RDX.

3. The adsorption processes on Mg(0001) are exothermic. The activation energy for **V4** configuration is as small as 2.5 kJ mol^{-1}. However, the activation energies of other configurations are too much, in the range of 964.9–1375.1 kJ mol^{-1}.
4. As compared to previous work [10], Mg powder is more active than Al powder, and Mg powder performs better in increasing the combustion exothermicity of RDX as well.

Acknowledgments We gratefully acknowledge the funding provided by the Laboratory of Science and Technology on Combustion and Explosion (Grant No. 9140C3501021101) for supporting this work. C.-C.Y. thanks the Innovation Project for Postgraduates in Universities of Jiangsu Province (Grant No. CXZZ13_0213) and the Innovation Foundation from the Graduate School of NJUST for partial financial support.

References

1. Dreizin EL, Berman CH, Vicenzi EP (2000) Combust Flame 122:30–42
2. Koch EC (2005) Propell Explos Pyrot 30:209–215
3. Wang RH, Guo Y, Sa R, Shreeve JM (2010) Chem-Eur J 16:8522–8529
4. Singh RP, Shreeve JM (2011) Chem-Eur J 17:11876–11881
5. Rajagopal C, Bhatt A, Kumar B, Saxena N (2009) Hazard and safety analysis for fuel rich propellant processing facility. In: Li SC (ed) Theory and practice of energetic materials. Science Press, Beijing, pp 590–600
6. Zhang J, Zhou DW, Huang YN, Peng P, Liu JS (2009) Rare Metal Mat Eng 38:1518–1525
7. Nobuhara K, Kasai H, Dino WA, Nakanishi H (2004) Surf Sci 566:703–707
8. Ye CC, Ju XH, Zhao FQ, Xu SY (2012) Chinese J Chem 30:2539–2548
9. Zhou SQ, Zhao FQ, Ju XH, Cheng XC, Yi JH (2010) J Phys Chem C 114:9390–9397
10. Ye CC, Zhao FQ, Xu SY, Ju XH (2013) J Mol Model 19:2451–2458
11. Tian K, Tu XY, Dai SS (2007) Surf Sci 601:3186–3195
12. Alfonso DR (2008) Surf Sci 602:2758–2768
13. Alfonso DR, Cugini AV, Sorescu DC (2005) Catal Today 99:315–322
14. Segall MD, Lindan PJD, Probert MJ, Pickard CJ, Hasnip PJ, Clark SJ, Payne MC (2002) J Phys Condens Matter 14:2717–2744
15. Perdew JP, Jackson KA, Pederson MR, Singh DJ, Fiolhais C (1992) Phys Rev B 46:6671–6687
16. Vanderbilt D (1990) Phys Rev B Condens Matter 41:7892–7895
17. Perdew JP, Burke K, Ernzerhof M (1996) Phys Rev Lett 77:3865–3868
18. Kresse G (1996) Phys Rev B 54:11169–11186
19. Fischer TH, Almlof J (1992) J Phys Chem 96:9768–9774
20. Amonenko VM, Ivanov VY, Tikhinskij GF, Finkel VA (1962) Phys Met Metallogr 14:47–51
21. Cronacher H, Heinz K, Müller K, Xu M-L, Van Hove MA (1989) Surf Sci 209:387–400
22. Bungaro C, Noguera C, Ballone P (1997) Phys Rev Lett 79:4433–4436
23. Hakey P, Ouellette W, Zubieta J, Korter T (2008) Acta Crystallogr Sect E 64:o1428
24. Halgren TA, Lipscomb WN (1977) Chem Phys Lett 49:225–232